An Improved Finite Element Method Formulation for the Analysis of Nonlinear Anisotropic Dielectric Waveguides

Stefano Selleri and Maurizio Zoboli, *Member, IEEE*

***Abstract*—An efficient and accurate vectorial finite element formulation is presented for the analysis of dielectric waveguides with arbitrary cross-sections, nonlinear behaviors, and anisotropic materials. Remarkable improvements in solution precision and computational effort have been obtained by evaluating new coefficients used in the matrix assembling procedure of the method. The influence of the mesh division is discussed and comparison with a scalar finite element approach is reported.**

I. Introduction

DIELECTRIC waveguides are fundamental components of optoelectronic and microwave devices and, as such, a rigorous description of the electromagnetic field propagating in these structures is essential. New fabrication technologies have provided devices with more and more complicate geometries which, together with the usage of anisotropic (i.e. $LiNbO_3$ and $LiTaO_3$) or lossy materials, considerably complicate any theoretical electromagnetic analysis. Furthermore, in the last years, nonlinear media have been object of great interest in order to realize devices with a large range of all-optical potential applications [1], [2]. For this kind of structures analytical approaches are possible only in particular cases [3], and therefore the demand for accurate and powerful numerical modeling techniques is constantly increasing. The Finite Element Method (FEM) has provided an ideal tool for this analysis, being easily applicable to structures with arbitrary geometries, nonlinear behaviors, anisotropic and lossy materials.

Nevertheless particular attention must be paid when this approach is used. Like all numerical techniques, the method divides the domain of interest into subregions forming a mesh, where the unknown field distribution will be sampled. Several studies have been carried out to test the result sensibility with respect to the domain division, especially in the linear case. Generally, the usage of dense meshes assures the result correctness. Nevertheless an excessive number of nodal points can be useless and even deleterious for computing efforts. For what concerns nonlinear structures, much more care must be exercised. In fact, as the material nonlinearities may produce strong refractive index changes and consequently strong variations in the unknown field, a particularly thick and accurate sampling is mandatory. On the contrary, as the iterative procedure usually developed for the nonlinear analysis remarkably increases the computing time, mesh dimensions must not be superfluously expanded. Adaptative mesh technique [4]–[6] seemed to be an ideal approach to overcame the question but, up to date, no exhaustive thorough examinations have been proposed for the nonlinear electromagnetic analysis. Recently Hayata *et al.* [7] have shown the great difference arising in the solutions of a nonlinear rectangular waveguide using a coarse or a refined mesh. Wang *et al.* [8] have discussed the same problem addressing some precautional factors to be applied in nonlinear numerical simulations. Nonetheless no definitive considerations have been suggested to choose adequate element sizes.

In this work a new efficient FEM formulation is presented in order to bring forward a contribution to the question. Its major feature, compared with previous approaches, regards the remarkable increase in the nonlinear solution accuracy and in the convergence speed for a fixed mesh, or, on the other hand, the reduction of the total nodes necessary to obtain a given precision.

These improvements have been possible by developing new matrix elements to be used in the assembling procedure of the nonlinear system matrices. Similar elements have been already evaluated for the simple quasi-two-dimensional problem (one transverse spatial variable) [9], and advantages related to their application have been already discussed [10]. A further contribution of this paper regards their expressions provided for quasithree-dimensional problems (two transverse spatial variables).

The next section deals with the proposed formulation and with the definition of the new matrix elements. Section III presents some applications in order to verify the achieved improvements and to compare solutions with those obtained by means of a scalar finite element formulation [11]. Conclusions follow.

II. Finite Element Theory

Supposing a time dependence of the magnetic field $\bar{H}$ expressed through the factor $e^{j(\omega t-\beta z)}$, ω and β being the angular frequency and the phase constant, the finite element method formulation usually starts from the so called curl-curl

Manuscript received May 12, 1994; revised August 2, 1994. This work was supported in part by the Italian Ministry for the University and the Scientifical and Technological Research, and by the Italian National Research Council.

The authors are with the Dipartimento di Ingegneria dell'Informazione, Parma University, 43100 Parma, Italy.

IEEE Log Number 9408581.

[12]–[15]

$$\bar{\nabla} \times ([\hat{\epsilon}]^{-1}\bar{\nabla} \times \bar{H}) - k_0^2 \bar{H} = 0 \tag{1}$$

where $[\hat{\epsilon}]$ and k_0 are respectively the nonlinear relative permittivity tensor and the wavenumber in vacuum. The formulation expressed by (1) is particularly suitable for dielectric waveguides as the field components of $\bar{H}$ are continuous across the dielectric interface. Consider a nonlinear medium with a diagonal permittivity tensor

$$[\hat{\epsilon}] = \begin{bmatrix} \epsilon_x & 0 & 0 \\ 0 & \epsilon_y & 0 \\ 0 & 0 & \epsilon_z \end{bmatrix}.$$

Its elements can be expressed as follows:

$$\begin{aligned} \epsilon_x &= \epsilon_l + \alpha f(E_x) + \eta f(E_y) + \eta f(E_z) \\ \epsilon_y &= \epsilon_l + \eta f(E_x) + \alpha f(E_y) + \eta f(E_z) \\ \epsilon_z &= \epsilon_l + \eta f(E_x) + \eta f(E_y) + \alpha f(E_z). \end{aligned} \tag{2}$$

In (2) ϵ_l is the linear (low power) permittivity; α is a parameter related to the so called Kerr coefficient $\bar{n}_2$ through $\alpha = c_0\epsilon_0\epsilon_l\bar{n}_2$ where c_0 and ϵ_0 are the light speed and the permittivity in the vacuum; the coefficient η depends on the particular nonlinear mechanism. The function $f(E)$ represents a given permittivity electric field dependence. For a Kerr-like material $f(E)$ is defined as $|E|^2$ while considering saturable models, which appear to be physically necessary when strong self-focusing with a quasithree dimensional formulation is simulated [8], $f(E)$ can be assumed to be

$$f(|E|) = \Delta\epsilon_{\text{sat}}[1 - e^{-\gamma|E|^2/\Delta\epsilon_{\text{sat}}}] \tag{3}$$

$\Delta\epsilon_{\text{sat}}$ being the maximum nonlinear permittivity increase and γ a coefficient depending on the particular nonlinear mechanism.

Dividing the domain of interest into second order triangular elements, the application to (1) of a Galerkin procedure based on the penalty function method [13] yields the following eigenvalue problem [15]:

$$([S] + [U])\{H\} - k_0^2[T]\{H\} = 0, \tag{4}$$

$\{H\}$ being the vector of the magnetic field nodal values. $[T]$ is a real symmetric matrix; for loss-free materials $[U]$ is a real symmetric matrix while $[S]$ a complex hermitian one. It is important to point out that only $[S]$ depends on the nonlinear permittivity tensor; $[S]$ is defined as follows:

$$[S] = \sum_{\Omega_e} \int\int_{\Omega_e} [B]^*[\hat{\epsilon}]^{-1}[B]^T d\Omega_e \tag{5}$$

where Ω_e refers to the current element of the domain and

$$[B] = \begin{bmatrix} \{0\} & -j\beta\{N\} & -\{N\}_y \\ j\beta\{N\} & \{0\} & \{N\}_x \\ j\{N\}_y & -j\{N\}_x & \{0\} \end{bmatrix}. \tag{6}$$

In (6) $\{N\}_x = \partial\{N\}/\partial x$, $\{N\}_y = \partial\{N\}/\partial y$ and $\{N\} = (N_1, N_2, N_2, N_4, N_5, N_6)^T$, $N_i (i = 1 \cdots 6)$ being the second order shape functions [15]. In particular $[S]$ can be considered a block matrix made up by the submatrices $[s_{xx}]$, $[s_{xy}]$, $[s_{xz}]$, $[s_{yx}]$, $[s_{yy}]$, $[s_{yz}]$, $[s_{zx}]$, $[s_{zy}]$ and $[s_{zz}]$ as follows:

$$[S] = \begin{bmatrix} [s_{xx}] & [s_{xy}] & [s_{xz}] \\ [s_{yx}] & [s_{yy}] & [s_{yz}] \\ [s_{zx}] & [s_{zy}] & [s_{zz}] \end{bmatrix}. \tag{7}$$

Developing the matrix product in (5) it yields the explicit expressions of the elements of each submatrix

$$\begin{aligned} s_{xxij} &= \beta^2 b_{ij} + a_{ij} \\ s_{xyij} &= -e_{ij} \\ s_{xzij} &= \beta f_{ij} \\ s_{yxij} &= -e_{ij} \\ s_{yyij} &= \beta^2 b_{ij} + d_{ij} \\ s_{yzij} &= \beta c_{ij} \\ s_{zxij} &= \beta f_{ij} \\ s_{zyij} &= \beta c_{ij} \\ s_{zzij} &= a_{ij} + d_{ij} \end{aligned}$$

where

$$\begin{aligned} a_{ij} &= \int_{\Omega_e} q \frac{\partial N_i}{\partial y}\frac{\partial N_j}{\partial y} d\Omega_e \\ b_{ij} &= \int_{\Omega_e} q N_i N_j d\Omega_e \\ c_{ij} &= \int_{\Omega_e} q N_i \frac{\partial N_j}{\partial y} d\Omega_e \\ d_{ij} &= \int_{\Omega_e} q \frac{\partial N_i}{\partial x}\frac{\partial N_j}{\partial x} d\Omega_c \\ e_{ij} &= \int_{\Omega_e} q \frac{\partial N_i}{\partial x}\frac{\partial N_j}{\partial y} d\Omega_e \\ f_{ij} &= \int_{\Omega_e} q N_i \frac{\partial N_j}{\partial x} d\Omega_e \end{aligned} \tag{8}$$

with the subscripts i and j, from 1 to 6, referring to the nodal points of each triangle. In (8) the coefficient q represents the appropriate elements of $[\hat{\epsilon}]^{-1}$ which vary from element to element and also within an element, depending on the unknown field through (2). The obtained (4) is thus a nonlinear problem; in particular a nonlinear generalized eigenvalue problem whose eigenvalues and eigenvectors correspond to the wavenumber in vacuum k_0 and the magnetic field $\{H\}$ respectively. A self-consistent nonlinear solution can be obtained following an iterative procedure [16], [17]. In order to be successful, the spurious solutions must be eliminated; in the proposed formulation the penalty function approach has been adopted although its application introduces a slight error in the solution values. The procedure is as follows:

- Specify the input data: the frequency ν ($\omega = 2\pi\nu$) and the input power P.
- Resolve (4) obtaining $\{H\}$.
- Calculate the unknown electric field $\bar{E}$ through the Maxwell's equation

$$\bar{E} = [\hat{\epsilon}]^{-1}(\bar{\nabla} \times \bar{H})/j\omega. \tag{9}$$

Specifically, as the magnetic field is defined within each element in terms of its nodal values $\{H\}$ and of the shape functions $\{N\}$, the vector of the electric field nodal values $\{E\}$ can be expressed by:

$$\{E\} = [\hat{\epsilon}]^{-1}([B]^T\{H\}e^{-j\beta z})/j\omega. \tag{10}$$

- Calculate the modified permittivity tensor for each element of the domain through (2). In particular the new formulation proposed in this work defines and modifies the permittivity tensor in each nodal point of the domain. Implications of this choice will be discussed in the following.
- iterate the above procedure (second, third and fourth steps) until the solution converges within the desired criterion.

The evaluation of the vector $\{E\}$ (step three) and of the new permittivity profile (step four) are critical operations in order to obtain convergence to a correct solution. Although the unknown vector $\{H\}$ is evaluated in each point of the mesh, permittivity tensors $[\hat{\epsilon}]$ are usually defined on each mesh element rather than on mesh points. This choice implies that all the nodes belonging to the same triangle present the same nonlinear refractive index variation. The approximation introduced is particularly rough if coarse meshes are considered and causes a kind of filtering in the permittivity profile.

Furthermore, applying (2) to the mesh elements, a unique electric field value over each triangle must be defined while the vector $\{E\}$ of the electric field nodal values is given through (10). This unique value is then usually obtained either through an integral average over the current triangle or by considering the barycentric value of the electric field or by taking the quadratic average of the nodal electric field values. Whatever the choice, a further approximation is introduced.

A more rigorous and realistic approach can be followed defining a permittivity tensor in each mesh point instead of in each mesh element and further expanding all elements of $[\hat{\epsilon}]$, or their inverse, in terms of the shape functions of the current triangle

$$q_n = \{N\}^T\{q_n\}_e \tag{11}$$

$$\{q_n\}_e = [q_{1n}\ q_{2n}\ q_{3n}\ q_{4n}\ q_{5n}\ q_{6n}] \tag{12}$$

with $n = x, y, z$ and the indices $1, \ldots, 6$ referring to the element nodes. Substituting (11), (12) into (8), it yields the explicit forms of the coefficients to be used in defining the matrix $[S]$. Their complete symbolic expressions can be calculated by means of a general computer software system as, for example, *Mathematica* [18]. The same permittivity expansion (11), (12) can be exercised to obtain the power expression in terms of the coefficients (8).

III. Numerical Applications

In this section a linear strip of width w and height h, sitting on a nonlinear substrate and surrounded by a linear cladding is considered. A saturable nonlinear model and particular w and h values are assumed in order to test the obtained solutions and to compare the results with the scalar finite element approach proposed by Li *et al.* [11].

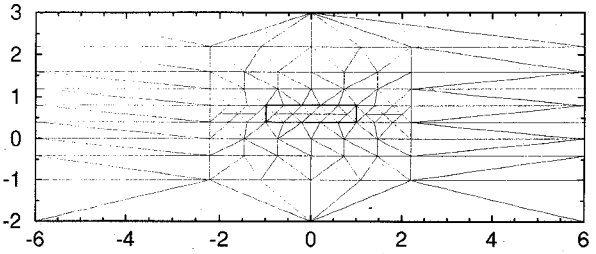

Fig. 1. Mesh A: $N_e = 166$; $N_p = 355$; $w = 2.0$ μm, and $h = 0.4$ μm.

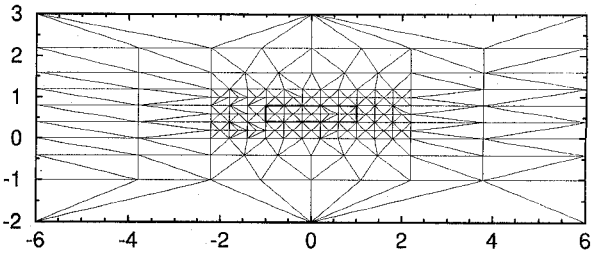

Fig. 2. Mesh B: $N_e = 334$; $N_p = 691$; $w = 2.0$ μm, and $h = 0.4$ μm.

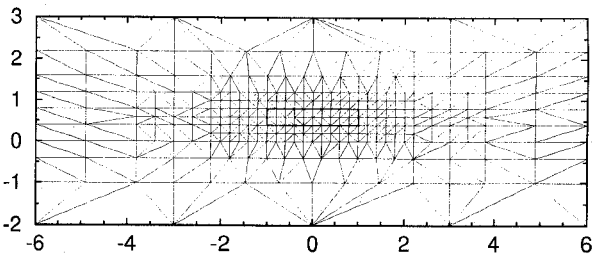

Fig. 3. Mesh C: $N_e = 566$; $N_p = 1159$; $w = 2.0$ μm, and $h = 0.4$ μm.

To analyze mesh influence, the waveguide cross-section has been divided into N_e elements with N_p total points. In particular $N_e = 166$ and $N_p = 355$ for mesh A in Fig. 1; $N_e = 334$ and $N_p = 691$ for mesh B in Fig. 2 and $N_e = 566$ and $N_p = 1159$ for mesh C in Fig. 3. All the considered meshes have been symmetrically made up with respect to the horizontal axis of the structure. Although computationally inefficient, this choice allows to concentrate better on the effects caused on the solutions by the number of nodes rather than by their distribution.

In the following examples, the values $w = 2.0$ μm, $h = 0.4$ μm, $n_{\rm co} = 1.57$, $n_{\rm cl} = 1.55$, $n_{\rm sb} = 1.55$, $\bar{n}_2 = 10^{-9}$m^2/W (MBBA liquid crystal), $\Delta\epsilon_{\rm sat} = 0.09696$, and the wavelength $\lambda = 0.515$ nm have been chosen.

It has been verified that the different element divisions strongly influence the final effective index $n_{\rm eff} = \beta/k_0$ and the field profile when using FEM formulations that define a constant permittivity tensor over each triangle. For example a formulation which evaluates the permittivity variations using the electric field integral average over the element has been considered. Results are reported in Fig. 4 where the normalized propagation constant $b = (n_{\rm eff}^2 - n_{\rm sb}^2)/(n_{\rm co}^2 - n_{\rm sb}^2)$ versus the input power has been plotted for the case of mesh A, together with some points of the dispersion curves related to mesh B and C. Solutions obtained with meshes A and B are comparable for very low powers, that is when

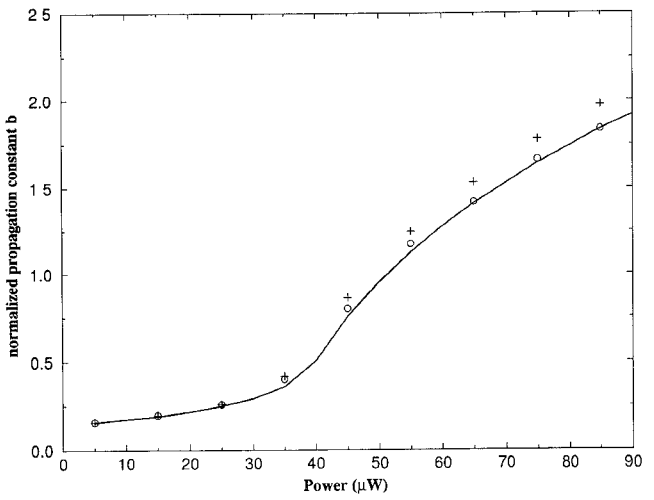

Fig. 4. Normalized propagation constant b versus the input power for mesh A (solid line), mesh B (circles), and mesh C (plus symbols), evaluating the permittivity variations through the electric field integral average over each triangle. Waveguide parameters: $w = 2.0$ μm, $h = 0.4$ μm, $n_{co} = 1.57$, $n_{cl} = 1.55$, $n_{sb} = 1.55$; nonlinearity parameters: $\bar{n}_2 = 10^{-9}$ m^2/W, $\Delta\epsilon_{sat} = 0.09696$, $\lambda = 0.515$ nm.

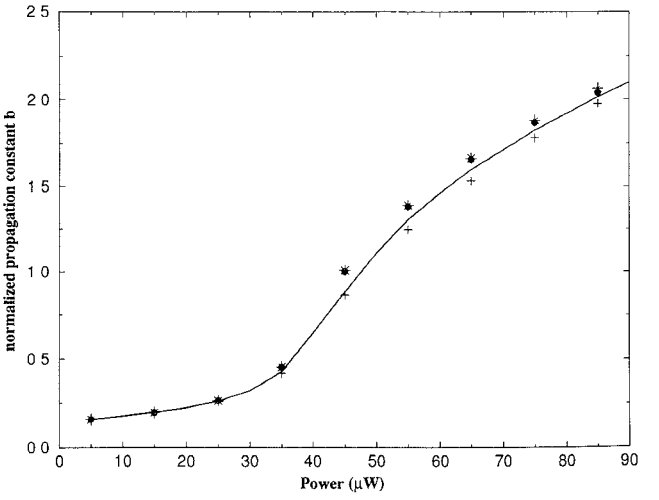

Fig. 5. Normalized propagation constant b versus the input power for mesh A (solid line), mesh B (black points), and mesh C (stars symbols), using the new formulation; the last curve of Fig. 4 is also reported (plus symbols). Waveguide and nonlinearity parameters as in Fig. 4.

the induced index changes are still much lower than the linear index difference $\Delta n = n_{co} - n_{cl}$, and for high power levels, i.e. when the saturation strongly affects the solutions. In the intermediate range, the agreement is lost and the effective indices of the finer mesh are higher than the other ones. Moreover, the division B seems to be not yet enough refined if compared with mesh C whose results are manifestly higher. A further increment in the element number of mesh C does not produce any significant variations. This circumstance allows the conclusion that the points of the last curve can be considered the superior limit of the solutions obtainable through this formulation. It is important to point out that these curves are quite different from the ones reported in [11]. Similar solution behaviors with respect to the meshes, can be observed also in FEM formulations which consider a constant permittivity tensor within the current triangle and approximate the electric field through the barycentric value or through the quadratic average of the nodal values. These examples clarify the imprecision and the solution uncertainty due to the usage of strong approximations like those previously explained.

Following the approach of section two, a remarkable improvement is achieved, as shown in Fig. 5. The solid line refers to solutions of mesh A. The normalized propagation constants lying on this curve present values even higher than the ones obtained with mesh C using the previous formulation. To facilitate the comparison, the solutions plotted in Fig. 4 with plus symbols are also reported in Fig. 5. The new formulation results for the other two structures are also plotted. Again the b values increase by refining the element division but now the two curves almost coincide as mesh C yields only very slight variations with respect to mesh B. Such a fine division is now useless and computationally inefficient as the same accuracy is attainable with less points.

A comparison between the usual and the new formulation emphasizes the better agreement of the latter with the scalar approach results proposed in [11] also considering not very fine meshes. Moreover it is worth pointing out that the vectorial approach provides an effective index slightly lower than the scalar one. Similar results have already been verified in previous works [16].

The effects of the new formulation can be observed also in the spatial distribution of the electromagnetic field. For example, the main components of the vector $\bar{H}$, computed for an input power $P = 55$ μW, obtained from the old and the new formulation, are shown in Figs. 6 and 7. It is interesting to observe that the new approach provides a field whose profile is slightly more focused and more displaced in the nonlinear substrate than the other one. This phenomenon can be explained as follows: as the formulation that evaluates the electric field through an integral average over the current triangle defines a permittivity tensor in each element, the nonlinear evolution of the refractive index profile is filtered and attenuated. On the contrary, defining a permittivity tensor in each node of the mesh, the refractive index can follow the nonlinearity law, point by point. This feature eliminates any filtering action thus providing more focused field distributions as well as higher propagation constants. It is important to note that this effect is independent of the element size since the same mesh has been used.

In terms of computing efforts, a further and important advantage has also been reached in the convergence speed of the nonlinear iterative process. Fig. 8 reports the normalized propagation constant versus the iteration number computed for a waveguide with $w = 2.0$ μm and $h = 1.2$ μm. The new formulation (curve a) is compared with three different approaches that evaluate the electric field over each element as follows: through an integral average (curve b); through a quadratic average of the $\{E\}$ values over each triangle nodes (curve c) and using the triangle barycentre value of the electric field (curve d). The improvement of the new formulation is evident both in terms of final normalized propagation constant and of convergence speed. In fact, the number of iterations needed to reach a stable solution is manifestly lower for curve

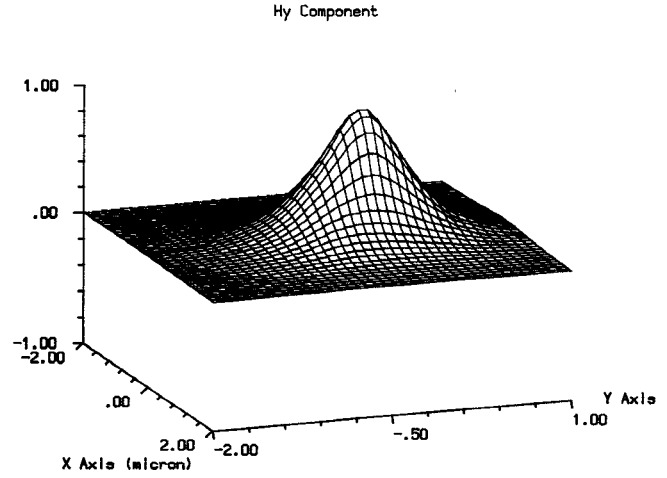

Fig. 6. The main component of the magnetic field for $P = 55$ μW; $\bar{n}_2 = 10^{-9}$ m^2/W, $\Delta\epsilon_{\rm sat} = 0.09696$. Mesh C has been considered. The permittivity variation has been evaluated using the electric field integral average over each triangle.

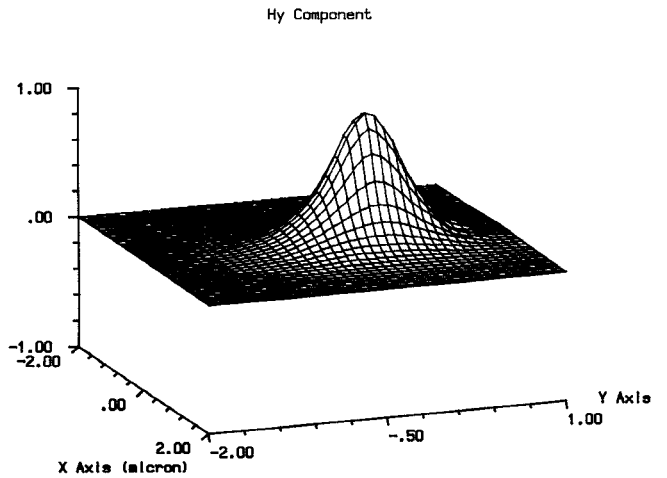

Fig. 7. The main component of the magnetic field for $P = 55$ μW; $\bar{n}_2 = 10^{-9}$m^2/W, $\Delta\epsilon_{\rm sat} = 0.09696$. Mesh C has been considered. The new formulation has been used.

a than for the others curves; furthermore only the final value of the former presents a good agreement with the results presented in [11]. On the contrary, the other formulations lead to different solutions as the third and fourth steps of the nonlinear procedure are not rigorously carried out.

IV. Conclusion

A new vectorial finite element method formulation for the analysis of quasithree-dimensional problems (two transverse spatial variables) has been proposed. Improvements related to the solution accuracy and computational effort have been achieved by developing new integral coefficients involved in the system matrix definition.

Some approximations related to the evaluation of the refractive index changes, commonly introduced in nonlinear FEM iterative procedure, have been discussed and eliminated. The solution accuracy thus reached is now mainly affected by the

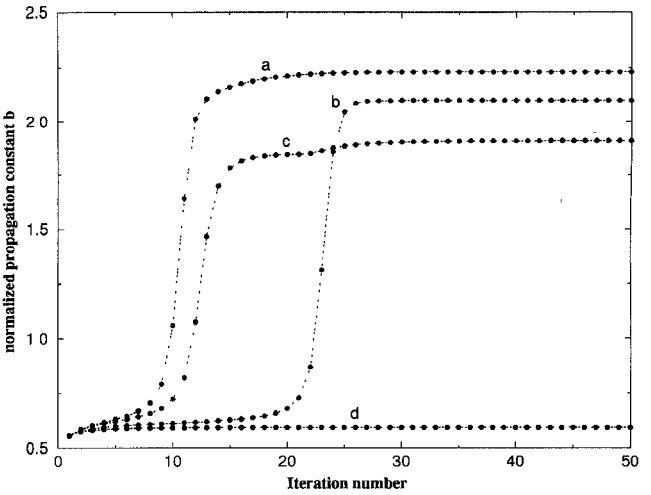

Fig. 8. Normalized propagation constant versus the iteration number. Comparison of the new formulation (curve a) with three different approaches that evaluate the electric field over each element through an integral average (curve b); through a quadratic average of the $\{E\}$ values over each triangle nodes (curve c) and using the triangle barycentre value of the electric field (curve d). Waveguide parameters: $w = 2.0$ μm, $h = 1.2$ μm, $n_{\rm co} = 1.57$, $n_{\rm cl} = 1.55$, $n_{\rm sb} = 1.55$. A saturable nonlinearity with $\bar{n}_2 = 10^{-9}$ m^2, $\Delta\epsilon_{\rm sat} = 0.09\ 696$, a wavelength $\lambda = 0.515$ nm, and an input power $P = 100$ μW have been considered.

presence of the penalty function. In order to overcame this effect and to avoid spurious modes, the application of this new approach to a transverse magnetic field [19]–[21] or to an edge elements FEM formulation will be object of future work.

References

[1] G. I. Stegeman, E. M. Wright, N. Finlayson, R. Zanoni, and C. T Seaton, "Third order nonlinear integrated optics," *J. Lightwave Technol.*, vol. LT-6, pp. 953–970, June 1988.

[2] G. I. Stegeman and R. H. Stolen, "Waveguides and fibers for nonlinear optics," *J. Opt. Soc. Am. B*, vol. 6, pp. 652–662, Apr. 1989.

[3] C. T Seaton, J. D. Valera, R. L. Shoemaker, G. I. Stegeman, J. T. Chilwell, and S. D. Smith, "Calculations of nonlinear TE waves guided by thin dielectric film bounded by nonlinear media," *IEEE, J. Quantum Electron.*, vol. QE-21, pp. 774–783, July 1985.

[4] J. Penman and M. D. Grieve, "Self-adaptive mesh generation technique for the finite element method," *IEE Proc.*, vol. 134, no. 8, pp. 634–650, Sept. 1987.

[5] O. C. Zienkiewicz and J. Z. Zhu, "Adaptivity and mesh generation," *Int. J. Numer. Methods Eng.*, vol. 32, special issue no. 4, pp. 783–810, Sept. 1991.

[6] R. D. Ettinger, F. A. Fernandez, and J. B. Davies, "Application of adaptative remeshing techniques to the finite element analysis of nonlinear optical waveguides," in *Int. Conf. Directions in Electromag. Wave Modeling Dig.*, New York, Oct. 1990, p. 48.

[7] K. Hayata and M. Koshiba, "Self-localization and spontaneous symmetry breaking of optical fields propagating in strongly nonlinear channel waveguides: limitations of the scalar field approximation," *J. Opt. Soc. Am. B*, vol. 9, pp. 1362–1368, Aug. 1992.

[8] X. H. Wang and G. K. Cambrell, "Simulation of strong nonlinear effects in optical waveguides," *J. Opt. Soc. Am. B*, vol. 10, pp. 2048–2055, Nov. 1993.

[9] K. Hayata, M. Nagai, and M. Koshiba, "Finite element formalism for nonlinear slab-guided waves," *IEEE Trans. Microwave Theory Tech.*, vol. MTT-36, pp. 1207–1215, July 1988.

[10] R. Di Muro, M. Montagna, S. Selleri, and M. Zoboli, "An efficient vectorial finite element method formulation for the analysis of dielectric slab waveguides," to be submitted.

[11] Q. Y. Li, R. A. Sammut, and C. Pask, "Variational and finite element analyses of nonlinear strip optical waveguides," *Opt. Comm.*, vol. 94, pp. 37–43, Nov. 1992.

[12] A. Konrad, "Vector variational formulation of electromagnetic field in anisotropic media," *IEEE Trans. Microwave Theory Tech.*, vol. MTT-24, pp. 553–559, Sept. 1976.
[13] B. M. A. Rahman and J. B. Davies, "Penalty function improvement of waveguide solution by finite elements," *IEEE Trans. Microwave Theory Tech.*, vol. MTT-32, pp. 922–928, Aug. 1984.
[14] M. Koshiba, K. Hayata, and M. Susuki, "Improved finite element formulation in terms of the magnetic field vector for dielectric waveguides," *IEEE Trans. Microwave Theory Tech.*, vol. MTT-33, pp. 227–233, Mar. 1985.
[15] M. Zoboli and P. Bassi, "The finite element method for anisotropic optical waveguides," in *Anisotropic and Nonlinear Optical Waveguides*, G. Stegeman and C. G. Someda, Eds. Amsterdam, The Netherlands: Elsevier, 1992.
[16] M. Zoboli, F. Di Pasquale, and S. Selleri, "Full-vectorial and scalar solutions of nonlinear optical fibers," *Opt. Comm.*, vol. 97, pp. 11–15, Mar. 1993.
[17] M. Zoboli and S. Selleri, "Finite element analysis of TE and TM modes in nonlinear planar waveguides," *Int. J. Nonlinear Optics Phys.*, vol. 3, Jan. 1994.
[18] S. Wolfram, *Mathematica, A System for Doing Mathematics by Computer*, The Advanced Book Program. Redwood City, CA: Addison-Wesley, 1991.
[19] K. Hayata, M. Koshiba, M. Eguchi, and M. Suzuki, "Vectorial finite element method without any spurious solutions for dielectric waveguiding problems using transverse magnetic field component," *IEEE Trans. Microwave Theory Tech.*, vol. MTT-34, pp. 1120–1124, Nov. 1986.
[20] Y. Lu and F. A. Fernandez, "An efficient finite element solution of inhomogeneous anisotropic and lossy dielectric waveguides," *IEEE Trans. Microwave Theory Tech.*, vol. MTT-41, pp. 1215–1223, June/July 1993.
[21] Z. A. Abid, K. L. Johnson, and A. Gopinath, "Analysis of dielectric guides by vector transverse magnetic field finite elements," *J. Lightwave Technol.*, vol. LT-11, pp. 1545–1549, Oct. 1993.

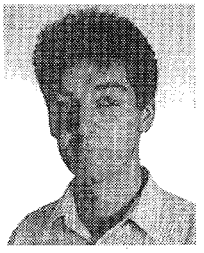

Stefano Selleri was born in Bologna, Italy, in 1966. He received the degree in electronic engineering from the Bologna University in 1991.

In 1992 he worked as a grant holder for the 'Centro Studi E Laboratori Telecomunicazioni' (CSELT) of Torino, Italy. Since Nov. 1992 he has been attending the doctoral studies at the Dipartimento di Ingegneria dell'Informazione of the University of Parma. His current research includes semiconductor laser, integrated optics, nonlinear optics and numerical methods for electromagnetic fields.

Mr. Selleri is a member of AEI.

Maurizio Zoboli (M'92) was born in Modena, Italy, in 1947. He graduated from the School of Engineering, University of Bologna, in December 1972.

From 1974 he worked in the Dipartimento di Elettronica Informatica e Sistemistica of the University of Bologna on theoretical and experimental characterization of optical waveguides. In 1979 became associate professor at the University of Bologna, teaching a course of electromagnetic fields and waves. In 1981 he was in the Computer Science of UCLA, Los Angeles, CA, where he is currently full professor, to work on optical fiber applications in Local Area Network. In 1991 he joined the Dipartimento di Ingegneria dell'Informazione of the University of Parma. His current research interests are in the field of optical communications, with special emphasis on optical fiber waveguide metrology and on numerical modeling of linear and nonlinear optical devices.

Mr. Zoboli is a member of AEI and OSA.